Proceedings of the 1st international Symposium on AI and Fluid Mechanics
Paper No S1 P1

Reconstruction of Flow Fields with Physics-Informed Neural Networks Based on Optimal Sensor Placement - Overview

Bingteng Sun[1], Shengze Cai[2], *Qiang Du[1,4,5,6], Lin Lu[3], Ruonan Wang[1], Shanyou Wang[1], Lei Xie[1], Renjie Xiao[7], Xiaokang Liu[8], Junqiang Zhu[1,6,7]

[1]*Advanced Gas Turbine Laboratory, Institute of Engineering Thermophysics, Chinese Academy of Sciences, Beijing, 100190, China*

[2]*College of Control Science and Engineering, Zhejiang University, Hangzhou, Zhejiang, 310027, China*

[3]*School of Computer Science and Technology, Shandong University, Qingdao, Shandong, 266237, China*

[4]*Qingdao Institute of Aeronautical Technology*

[5]*Nanjing Institute of Future Energy System Research*

[6]*National Key Laboratory of Science and Technology on Advanced Light-duty Gas-turbine, Beijing 100190, China*

[7]*University of Chinese Academy of Sciences, Beijing, 100190, China*

[8]*Visual Computing and Learning Lab, School of Intelligence Science and Technology, Peking University, Beijing, 100871, China*

Keywords: physics-informed neural networks; optimal sensor placement; flow field reconstruction

Abstract

High-fidelity flow field reconstruction has been a focal point for many research studies, as the measured sensor data are often sparse and incomplete in both time and space. Physics-informed neural networks (PINNs) have been proposed to reconstruct fields using imperfect data, as they incorporate physical principles and thereby reducing reliance on the known sensor data. However, the placement of sensors remains crucial for optimizing PINNs, and existing studies have not sufficiently considered this aspect. Therefore, developing algorithms that intelligently improve sensor placement is of significant importance. In this study, we introduce a general approach that employs differentiable programming with attention modules to optimize sensor placement within the training of a PINNs model in order to improve flow field reconstruction. We evaluate our method using the lid-driven cavity flow problem. The result indicates that our method improves test scores and effectively learns the optimal layout of sensors. This research advances our understanding of the relationship between sensor placement and predictive precision using PINNs, which will contribute to the development of fields such as health monitoring, data assimilation, and super-resolution reconstruction.

1. Introduction

Spatial fluid field reconstruction from limited local sensor information is a common problem in high-dimensional complex physical systems, some examples include cardiac blood flow modeling [1,2], ship wake identification [3], and climate science[4]. Traditional linear theory-based tools, including Galerkin transformations[5], Gappy proper orthogonal decomposition[6], and linear stochastic estimation methods such as Kalman filter (KF)[7], face challenges in reconstructing global fields from a limited number of sensors under those systems with complex physics. Moreover, with the widespread attention received by machine learning (ML), deep neural networks (DNN) have been regarded as promising nonlinear alternatives for reconstructing chaotic data from sparse measurements [8].Most of the existing methods for recovering high-resolution field from low-resolution data using deep learning methods come from Super-resolution (SR) [9], in which convolutional neural networks (CNN) are most used [10]. However, almost all practical experimental measurements and numerical simulations rely on unstructured grids or random

*Corresponding Author, Qiang Du duqiang@iet.cn

sensor placements. These grids are incompatible with CNN methods, which require the training data to be structured and uniformly arranged [11,12].

Physics-informed neural networks (PINNs), proposed earlier by Raissi et al. [13], have obtained popularity in the physical field prediction for outperformed capability and available physical interpretability, including forward [14,15,16] and inverse [17,18,19] problems. PINNs are usually regarded as simulation methods based on neural networks. JIN et al. [14] developed the Navier-Stokes flow nets (NSFnets) to solve the incompressible flow by considering two different mathematical formulations of the Navier-Stokes equations: the velocity-pressure (VP) formulation and the vorticity-velocity (VV) formulation. Cai et al. [20] indirectly calculated the velocity and pressure field by measuring the temperature field with to ographic background oriented schlieren. Further, Sun et al. [21] used PINNs to accurately calculate the ideal vascular flow without any simulation data, proving that PINN is a promising complement to traditional computational fluid dynamics (CFD) methods. However, the current PINN method performs poorly in solving highly nonlinear systems such as turbulent fields or three-dimensional scenes, so PINN at this stage should not only be treated it as a CFD method, but also paid more attention to its advantages in processing sparse data. Xu et al. [22] investigated the influence of different sparsity and different missing regions to field reconstruction with PINN and revealed that the proposed approach not only can reconstruct the true velocity field with high accuracy, but also can predict the pressure field precisely, even when the data sparsity reaches 1% or the core flow area data are truncated away. This study provides encouraging insights that the PINN can serve as a promising data assimilation method.

It is worth noting that no matter the linear theory-based tools, SR methods or PINNs, the location of the sparse points/sensor placement is crucial to the fidelity and efficiency of the field reconstruction. Various strategies have been proposed to optimize the location of sensors, i.e., optimal sensor placement (OSP) methods. Deng et al. [23] focused on the OSP strategy based on a DNN for turbulent flow recovery within the data assimilation framework of the ensemble Kalman filter (EnKF). Cai et al. [24] proposed an OSP method based on the PINN framework that selects sensor locations by evaluating residuals of governing equations. Sharma et al. [25] systematically generated 80 distinct sensor configurations for a 2-dimensional stenosis hemodynamics problem and demonstrated that the accuracy of flow-field predictions is notably more sensitive to sensors located close to the stenosis and inlet. We can see that the existing OSP methods are generally decoupled from the field reconstruction algorithm, so the optimization of sensor placements does not adaptively match the updates of the reconstruction model. In particular, the OSP algorithm combined with the PINN method is basically empirical.

In response to the aforementioned challenges, we propose a model that incorporates sparse sensor placement method into a PINN, called OSPPINN. OSPPINN enables to reconstruct a field by optimizing the sensors positions via backpropagation, thereby facilitating the model's exploration of the spatial domain and enhancing sensor positioning effectively. OSPPINN consists of three modules: Interpolator, Encoder, and Decoder, which are responsible for real-time acquisition of sensor values, sparse information attention feature extraction, and PDE solution respectively. The remainder of the paper is organized as follows: The OSPPINN method is introduced in Section 2. The proposed method is applied to the lid-driven cavity flow problem in comparison to the vanilla PINN and uniform sensor placement method in Section 3. The conclusions are provided in Section 4.

2. Numerical Method

2.1 Pinn-driven optimal sensor placement model (OSPPINN)

*Corresponding Author, Qiang Du duqiang@iet.cn

As shown in Figure 1 (a), the OSPPINN framework consists of three main components of its architecture: a sensor value Interpolator, a sensor data Encoder, and a PDE solver Decoder. The sensor value Interpolator is to get the property values for the variable sensor locations and maps spatial coordinates to encoding vectors. The sensor data attention-driven Encoder maps the sensor data, obtained by concatenating spatial encodings and property values, to a compressed latent matrix. The PDE solver Decoder is a physics-informed neural network that predicts the field value at any given residual position. In addition to the neural network's weights, the sensor positions are treated as trainable parameters within the model, which we aim to optimize for improved performance in subsequent Decoder solving.

Sensor value Interpolator. Following each optimization iteration, the sensor positions undergo dynamic adjustments, necessitating the recalibration of corresponding physical property values at updated coordinates. This recalculation process is seamlessly integrated into the overall network optimization workflow and must therefore be executed in a differentiable manner. To achieve this, we utilize a differentiable interpolation method to determine sensor values at arbitrary positions. Specifically, for the updated sensor locations at each step, we employ either bilinear or trilinear interpolation based on neighboring information to compute the property values. These interpolated sensor measurements, along with their positional coordinates, constitute the input tensor for the subsequent Encoder network. To ensure numerical stability during position updates, a boundary proximity constraint is enforced: sensors approaching computational domain boundaries trigger gradient sign inversion in their update direction vectors. This mechanism effectively repels sensors from boundary regions while maintaining differentiability throughout the optimization trajectory.

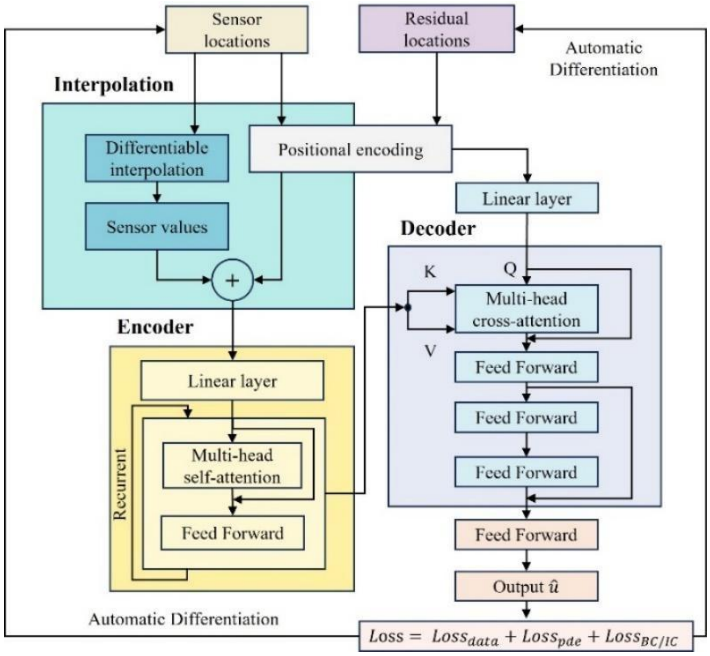

Figure 1 Details of the OSPPINN model, which includes Interpolator, Encoder and Decoder modules.

Sensor data Encoder. The Encoder module takes the locations and values of the sensors as inputs, which are processed through a fully connected linear layer to match the input dimensions required by the subsequent attention block. Each module contains a multi-head self-attention layer and a feedforward layer. The self-attention layer maintains the output dimensions consistent with the input, and we incorporate a residual connection around it to ensure that sensor information is fully preserved. The training of the

*Corresponding Author, Qiang Du duqiang@iet.cn

attention module is critical, as it determines the quality of the compressed representation, which in turn influences the optimization of the subsequent PDE solver Decoder.

PDE solver Decoder. In the Decoder block, the multi-head cross-attention allows residual points to be solved selectively focusing on specific dependencies within the input sensor compact representation during the decoding process, enabling it to capture more relevant useful information than conventional PINNs. The keys and values for this cross-attention are provided by the Encoder output, while the spatial vector, post-residual point position encoding, serves as the query array. Similar to the Encoder, we employ residual connections around the cross-attention layer. This is followed by three feed forward layers, which are similar to vanilla DNN PINNs used to learn the PDE solution of the residual point. The purpose of the Decoder module is to select appropriate sensor data for the specific residual point, facilitating its PINN solving process.

Sensor locations $\boldsymbol{S}$ along with OSPPINN's weights $\boldsymbol{W}$ and biases $\boldsymbol{b}$ need to be learned by solving an optimizing problem, defined as in equation (1).

$$\boldsymbol{W}, \boldsymbol{b}, \boldsymbol{S} = \underset{\boldsymbol{W},\boldsymbol{b},\boldsymbol{S}}{argmin}\, Loss \tag{1}$$

where $Loss$ is the objective function, which consists of the following three components

$$Loss = \lambda_{sensor} Loss_{sensor} + \lambda_{pde} Loss_{pde} + \lambda_{bc/ic} Loss_{bc/ic} \tag{2}$$

where $Loss_{sensor}$, $Loss_{pde}$ and $Loss_{bc/ic}$ represent the sensor data driven component, the physics-informed components in the interior domain and the initial/boundary conditions, respectively. λ_{sensor}, λ_{pde} and $\lambda_{bc/ic}$ are the corresponding weights for each component, set to 2, 0.2, and 2 in this work. The physics are encoded into the OPSPINN by penalizing the residuals of the PDEs over a set of collocation points in the interior and associated BC/ICs of a set of collocation points on the boundary. In this study, we use a fixed learning rate of 0.001 combined with the Adam method for training.

3. Results

3.1 The lid-driven cavity flow problem

In this case, we employ a canonical benchmark problem which is a well-established benchmark in PINN prediction, the steady-state flow in a two-dimensional lid-driven cavity, to analyse the performance of the OSPPINN. By comparing with the vanilla PINN and OSPPINN with fixed sensor locations, we demonstrate the effectiveness of sensor optimization and sensor data encoder. The performance of the trained models is assessed using the L_2 norm errors $\frac{\|y-\hat{y}\|_2}{\|y\|_2}$. The flow system is governed by the steady incompressible Navier–Stokes equation, which can be written as:

$$\begin{aligned} \boldsymbol{u}(x,y)\cdot\nabla\boldsymbol{u}(x,y) + \nabla p(x,y) - \frac{1}{Re}\Delta\boldsymbol{u}(x,y) = 0 \ (x,y)\in\Omega, \\ \nabla\cdot\boldsymbol{u}(x,y) = 0 \ (x,y)\in\Omega, \\ \boldsymbol{u}(x,y) = (1,0) \ (x,y)\in\Gamma_1, \\ \boldsymbol{u}(x,y) = (0,0) \ (x,y)\in\Gamma_0, \end{aligned} \tag{3}$$

*Corresponding Author, Qiang Du duqiang@iet.cn

where $\boldsymbol{u}(x,\ y)$ and $p(x,\ y)$ are the velocity vector field and the scalar pressure field, Re is the Reynolds number of the flow, $\Omega\ \in\ [0,\ 1]\ *\ [0,\ 1]$, and Γ_1 denotes the top boundary of the two-dimensional square cavity, Γ_0 denotes the other three sides. We conduct experiments 40 times using 2 sensors, 4 sensors and 6 sensors at $Re\ =\ 1000$ to study the prediction performance. The maximum iteration number is set to 10000, and the number of residual points for the PDE loss term is set to 2601. As exemplified in the representative training experiment shown in Figure 2, when the training epochs increase, the results of OSPPINN (fixed) and OSPPINN (moving) gradually converge and the relative errors obtained after reaching the final training epoch are $7.099\ \times\ 10^{-2}$, $5.984\ \times\ 10^{-2}$ using 4 sensors. The vanilla PINN hardly learns the flow field features and is therefore not shown in Figure 2. The parameters of the three models are basically the same.

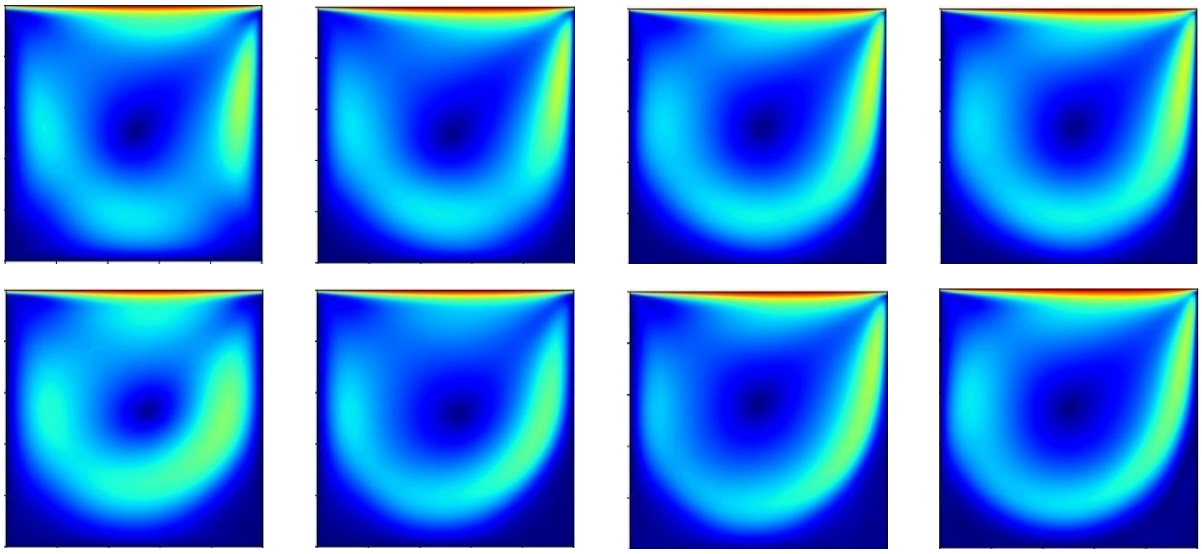

(a) (b) (c) (d)

Figure 2 Prediction of velocity magnitudes for the two-dimensional lid-driven cavity problem is shown for the following epochs: (a) epoch 2000, (b) epoch 4000, (c) epoch 8000, and (d) epoch 10000 at Re=1000 using 4 sensors, the corresponding models from top to bottom are OSPPINN (fixed) and OSPPINN (moving).

As shown in Figure 3 (a), when vanilla PINN uses sensor data to improve training accuracy, the relative errors are large and the results are unstable, which means that simply adding $Loss_{sensor}$ to the vanilla PINN's loss function does not significantly reduce the optimizing complexity. The Encoder module enables to adaptively decide how to extract the latent features of the sensors for the subsequent PDE Decoder, which results in a smoother response of the OSPPINN to changes in sensor positions, leading to a more stable training process. As expected, increasing the number of sensors the training performance improves. The moving sensor strategy highly improves the field reconstruction capability of the network, in terms of mean and standard deviation of the error distribution, as seen in the comparison of L_2 norm errors. The final sensor placements are shown in Figure 3 (b). The sensor locations are tuned in conjunction with the OSPPINN's trainable parameters and are primarily distributed in areas with a large gradient of flow field values. Figure 4 shows the feature maps of the multi-head cross attention module during one of the training sessions, with the attention weights averaged across the heads. A general trend is observed, the attention weight for each sensor increases as the distance to the sensor decreases, even though the sensor points are not strictly centered in the feature maps. This phenomenon occurs primarily because each sensor has already integrated information from other sensors by this stage of training.

*Corresponding Author, Qiang Du duqiang@iet.cn

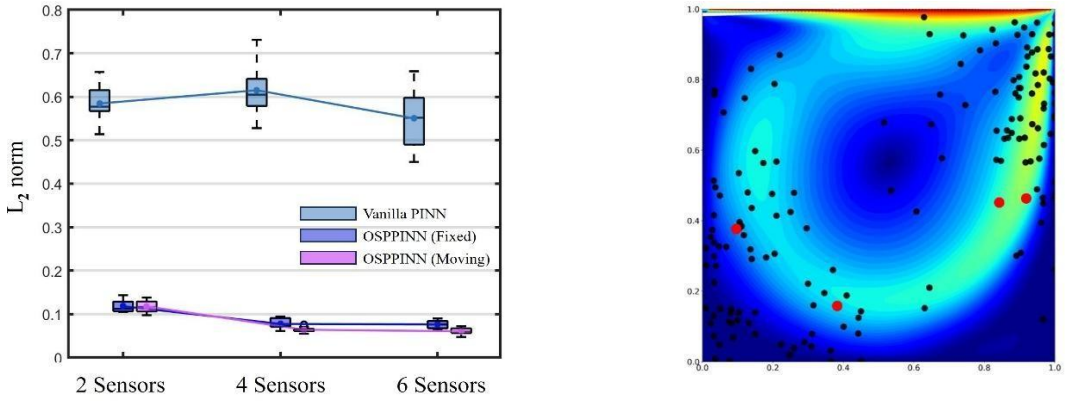

Figure 3 Prediction results of the two-dimensional lid-driven cavity problem (a) relative errors, (b) initial positions (red) and final position post-training (black) for the 4 sensors.

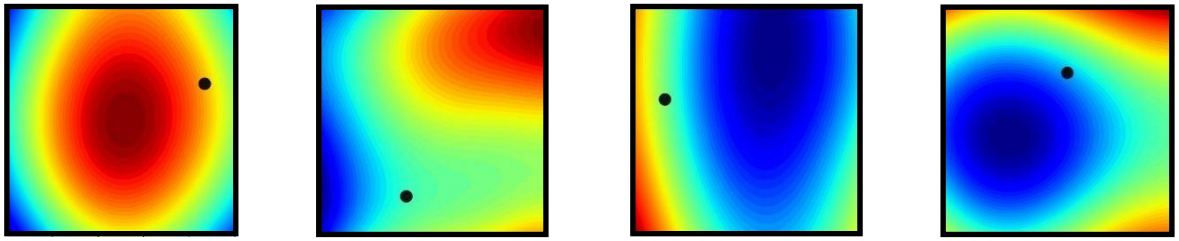

Figure 4 The feature maps of the multi-head cross attention module.

4. Conclusion

In this study, we introduce OSPPINN that employs differentiable programming with attention modules to exploit sensor placement in order to improve field reconstruction fidelity. We evaluate the inference ability of OSPPINN in the cylinder flow problem. Repeated experiments have proven that our method is effective and stable. The Interpolation module can adaptively update the sensor value in real time according to the change of sensor position, the Encoder module and Decoder module can more effectively use sensor information to improve the accuracy of PDE solution. This study innovatively combines PINN with OSP for data assimilation. Future work will consider combining the model in this study with traditional data assimilation methods, such as EnKF method or adjoint method.

Acknowledgments

The authors wish to acknowledge the financial support of the National Natural Science Foundation of China (NSFC) through the Basic Science Center Program (*GrantNo.*52488101), the National Science and Technology Major Project (J2019-III-0003-0046), and the cloud computing supported by the Beijing Super Cloud Computing Center. Meanwhile, the current work is also supported by the Taishan Scholars Program.

References

1. Yakhot A, Anor T, Karniadakis GE. A reconstruction method for gappy and noisy arterial flow data. IEEE Trans Med Imaging. 2007 Dec;26(12):1681-97. doi: 10.1109/tmi.2007.901991. PMID: 18092738.

*Corresponding Author, Qiang Du duqiang@iet.cn

2. Sankaran S, Esmaily Moghadam M, Kahn AM, Tseng EE, Guccione JM, Marsden AL. Patient-specific multiscale modeling of blood flow for coronary artery bypass graft surgery. *Annals of biomedical engineering.* 2012 Oct;40:2228-42.

3. Graziano, Maria Daniela, Marco D'Errico, and Giancarlo Rufino. Ship heading and velocity analysis by wake detection in SAR images. *Acta astronautica*. 128 2016: 72-82.

4. Kalnay, E. *Atmospheric Modeling, Data Assimilation and Predictability*. Vol. 341. Cambridge University Press, 2003.

5. Boisson, J. & Dubrulle, B. Three-dimensional magnetic field reconstruction in the VKS experiment through Galerkin transforms. *New J. Phys*. 13, 023037, 2011.

6. Bui-Thanh, T., Damodaran, M. & Willcox, K. Aerodynamic data reconstruction and inverse design using proper orthogonal decomposition. *AIAA J*. 42, 2004.

7. Suzuki, T. & Hasegawa, Y. Estimation of turbulent channel flow at $Re_\tau = 100$ based on the wall measurement using a simple sequential approach. *J. Fluid Mech.* 830, 760–796, 2006.

8. Brunton, S. L., Noack, B. R. & Koumoutsakos, P. Machine learning for fluid mechanics. *Annu. Rev. Fluid Mech*. 52, 477–508, 2020.

9. Shen, Yanqiong, Tao Jiang, and Chao Zhang. An Overview of Image Super-resolution Reconstruction. 2024 IEEE 6th Advanced Information Management, Communicates, *Electronic and Automation Control Conference (IMCEC).* Vol. 6. IEEE, 2024.

10. Fukami K, Maulik R, Ramachandra N, Fukagata K, Taira K. Global field reconstruction from sparse sensors with Voronoi tessellation-assisted deep learning. Nature Machine Intelligence. 2021 Nov;3(11):945-51.

11. LeCun, Y., Bottou, L., Bengio, Y. & Haffner, P. Gradient-based learning applied to document recognition. *Proc. IEEE* 86, 2278–2324, 1998.

12. Fukami, K., Fukagata, K. & Taira, K. Super-resolution reconstruction of turbulent flows with machine learning. *J. Fluid Mech.* 870, 106–120, 2019.

13. M. Raissi, P. Perdikaris, and G. E. Karniadakis, Physics-informed neural networks: A deep learning framework for solving forward and inverse problems involving nonlinear partial differential equations, *J. Comput. Phys.* 378, 686, 2019.

14. X. Jin, S. Cai, H. Li, and G. E. Karniadakis, NSFnets (Navier-Stokes flow nets): Physics-informed neural networks for the incompressible Navier-Stokes equations, *J. Comput. Phys.* 426, 109951, 2021.

15. R. Laubscher, Simulation of multi-species flow and heat transfer using physics-informed neural networks, *Phys. Fluids* 33, 087101, 2021.

16. H. Gao, L. Sun, and J. X. Wang, Super-resolution and denoising of fluid flow using physics-informed convolutional neural networks without high-resolution labels, *Phys. Fluids* 33, 073603, 2021.

*Corresponding Author, Qiang Du duqiang@iet.cn

17. Y. Chen, L. Lu, G. E. Karniadakis, and L. Dal Negro, Physics-informed neural networks for inverse problems in nano-optics and metamaterials, *Opt. Express* 28, 11618, 2020.

18. S. Mishra, and R. Molinaro, Estimates on the generalization error of physics-informed neural networks for approximating a class of inverse problems for PDEs, *IMA J. Numer.* Anal. 42, 981, 2022.

19. X. Chen, L. Yang, J. Duan, and G. E. Karniadakis, Solving inverse stochastic problems from discrete particle observations using the Fokker-Planck equation and physics-informed neural networks, *SIAM J. Sci. Comput.* 43, B811, 2021.

20. S. Cai, Z. Wang, F. Fuest, Y. J. Jeon, C. Gray, and G. E. Karniadakis, Flow over an espresso cup: Inferring 3-D velocity and pressure fields from tomographic background oriented Schlieren via physics informed neural networks, *J. Fluid Mech.* 915, A102, 2021.

21. Sun L, Wang JX. Physics-constrained bayesian neural network for fluid flow reconstruction with sparse and noisy data. *Theoretical and Applied Mechanics Letters.* 2020 Mar 1;10(3):161-9.

22. Xu S, Sun Z, Huang R, Guo D, Yang G, Ju S. A practical approach to flow field reconstruction with sparse or incomplete data through physics informed neural network. *Acta Mechanica Sinica.* 2023 Mar;39(3):322302.

23. Deng, Zhiwen, Chuangxin He, and Yingzheng Liu. Deep neural network-based strategy for optimal sensor placement in data assimilation of turbulent flow. *Physics of Fluids* 33.2, 2021.

24. Cai S, Wang Z, Wang S, Perdikaris P, Karniadakis GE. Physics-informed neural networks for heat transfer problems. *Journal of Heat Transfer.* 2021 Jun 1;143(6):060801.

25. Sharma Y, Tyagi A, Kumar G, Singh RK. Comparative Analysis of Sensor Configurations for Blood Flow Predictions via Physics-Informed Neural Networks. *In2024 4th International Conference on Innovative Practices in Technology and Management (ICIPTM)* 2024 Feb 21 (pp. 1-6). IEEE.

*Corresponding Author, Qiang Du duqiang@iet.cn